forests

MDPI

Article

The Gradient Variation of Location Distribution, Cross-Section Area, and Mechanical Properties of Moso Bamboo Vascular Bundles along the Radial Direction

Hongbo Li [1,2,*], Qipeng Zhu [1], Pengchen Lu [1], Xi Chen [1] and Yu Xian [3]

[1] College of Agricultural Engineering, Shanxi Agricultural University, Jinzhong 030801, China; s20212062@stu.sxau.edu.cn (Q.Z.); s20222074@stu.sxau.edu.cn (P.L.); 20233033@stu.sxau.edu.cn (X.C.)

[2] Dryland Farm Machinery Key Technology and Equipment Key Laboratory of Shanxi Province, Jinzhong 030801, China

[3] College of Forestry, Shanxi Agricultural University, Jinzhong 030801, China; xianyu@sxau.edu.cn

* Correspondence: lihb@sxau.edu.cn; Tel.: +86-135-9310-0742

Abstract: Bamboo is a typical natural fiber-reinforced composite with excellent mechanical properties, which are determined by its special micro-structure. As the reinforcing phase, the vascular bundles play a central role in the control of the mechanical properties of bamboo macro-structure. To find the exact gradient variation of the mechanical properties of these continuously distributed vascular bundles within the bamboo culm, 4-year-old Moso bamboo was chosen to investigate the variation of locate-distribution, cross-section area, and mechanical properties of single vascular bundles along the longitudinal and radial directions with respect to their location from the base, middle, and top sections of bamboo culm, respectively. It shows that the spatial distribution of vascular bundles along the column is distributed exponentially from the inside to the outside of the culm. The cross-section area of the vascular bundles decreased exponentially from the inside to the outside along the radial direction. All the vascular bundles were then carefully separated from bamboo strips and tested via the tensile tests. Test results show that the longitudinal tensile strengths of vascular bundles ranged from 180.44 to 774.10 MPa, and the longitudinal Young's modulus ranged from 9.00 to 44.76 GPa. The tensile strength of vascular bundles at the outer side was three times higher than that of the inner side, while Young's modulus at the outer side was three to four times higher than that of the inner side. For all three height positions, the strengths and Young's modulus of vascular bundles are all exponentially increased from the inner side to the outer side along the radial direction. This work will provide a basis for the highly processed product's application of bamboo resources and a reference for further study on the trans-scale analysis of the mechanical properties of bamboo.

Keywords: Moso bamboo; vascular bundle; functionally graded material; mechanical properties

Citation: Li, H.; Zhu, Q.; Lu, P.; Chen, X.; Xian, Y. The Gradient Variation of Location Distribution, Cross-Section Area, and Mechanical Properties of Moso Bamboo Vascular Bundles along the Radial Direction. *Forests* **2024**, *15*, 1023. https://doi.org/10.3390/f15061023

Academic Editor: Alain Cloutier

Received: 16 May 2024
Revised: 5 June 2024
Accepted: 7 June 2024
Published: 13 June 2024

1. Introduction

As renewable resources and grows throughout the world's tropical and subtropical regions, bamboo has a long and well-established tradition as a traditional material used in various aspects of life and production, such as household materials, furniture, crafts, paper, and textiles. Compared with the rich resources of bamboo, the available wood supply is decreasing quickly. To relieve the supply and demand stresses in wood resources, public attention has turned to bamboo as an alternative raw material for wood products. At the same time, plastic waste pollution is another serious environmental pollution crisis on Earth. To reduce plastic pollution and address climate change, researchers have tried many methods to find candidates to replace plastic products. Bamboo, recognized as a natural and renewable biomass material [1], emerges as an ideal alternative to plastic. An initiative of "bamboo as a substitute for plastic" was proposed in 2022 [2].

Among the typical natural biological composite, bamboo has one of the most favorable combinations of low density and high mechanical strength [3]. Its specific properties are comparable with conventional materials such as low-carbon steel and glass-reinforced plastics [3,4], which made it one of the best raw materials in Southeast Asia for the construction of scaffolding, packing boards, and furniture panels. As a biological material, bamboo exhibits many levels of hierarchical structures, from subcells, cells, and tissue to macroscopic plant bodies [5–7]. Its exceptional mechanical properties are determined by its unique macroscopic (bamboo culm), mesoscale (vascular bundles), microscopic (fibers), and nanoscopic (microfibril) structures [8–11].

Along the bamboo culm cross-section, it can be observed that the vascular bundles are distributed non-uniformly through the culm thickness. Most of the vascular bundles are concentrated densely near the exterior periphery while distributed sparsely near the inner zone. With the vascular bundles' volume density, type, and size spatially varying continuously, the bamboo's macroscopic structure possesses a continuously graded mechanical property. So, the bamboo structure is viewed as a natural functional graded composite material [11–14].

To investigate the distribution regularity of bamboo's mechanical properties along the culm thickness, bamboo slices were split and tested via tensile tests. For tensile strength and Young's modulus of bamboo culm, test results showed that although both of them were increased continuously from the inner side to the outer side, the gradient regularity was not consistent in the same way [15–18]. For Moso bamboo, Amada et al. [15,16] got the strength and Young's modulus increased parabolically, and Li and Shen [17] regarded Young's modulus increased cubically, while Nogata and Takahashi [18] found the strength and Young's modulus increased exponentially with radial distance.

Bamboo is a typical natural fiber-reinforced composite. Its gradient mechanical properties are determined by its special micro-structure. As the reinforcing phase, the vascular bundles play a central role in the appearance of bamboo culm with its number, shape, size, content, and mechanical properties [19–21].

Research showed that the distribution of vascular bundles volume fraction along the radial direction may follow different forms, namely linear [17], quadratic [13], or exponential curve [22]. Using an image binarization method based on the K-means clustering algorithm, Xu et al. [14,23] found that the vascular bundles' volume fraction of Moso bamboo [*Phyllostachys edulis*] decreased exponentially, the length-to-width ratio of vascular bundle decreased quadratically, and the width of vascular bundle increased linearly along the radial direction from the outer side to the inner side.

The bamboo vascular bundle is hard but tiny, with its diameter ranging between 100 and 500 μm. The strong adhesive between rigid vascular bundles and their surrounding parenchyma matrix made it very difficult to directly separate intact vascular bundles from bamboo slices with enough length. To obtain a better and more comprehensive understanding of the mechanical behavior of bamboo vascular bundles, many isolation techniques, such as mechanical [4,24,25], chemical [17,26], or biological [27] treatment methods, were used to extract vascular bundles from bamboo culm. Osorio et al. [4] developed a novel mechanical extraction and obtained strength values. Young's modulus of vascular bundles of the bamboo species *Guadua angustifolia* were 800 MPa and 43 GPa, respectively. Wang and Shao [24] extracted vascular bundles of Moso bamboo by handwork and obtained the average tensile strength and Young's modulus with 523.2 MPa and 22.3 GPa, respectively. The mechanical process can separate bamboo vascular bundles effectively. However, the extracted vascular bundles can be damaged due to the strong rigidity of the bamboo culm.

Compared to the mechanical method, the chemical isolation technique could produce more intact vascular bundles [28]. For example, Li and Shen [17] separated vascular bundles of Moso bamboo from three height positions with an alkali treatment method and tested the tensile strength varied from 495.2 to 916.2 MPa, and Young's modulus varied from 17.0 to 35.9 GPa. Also, they pointed out that both the tensile strength and Young's modulus were linearly increased from the inner zone to the outer surface. Recently, Li et al. [26] reported a top-down strategy by using a two-step process involving chemical delignification and air-drying to extract high-performance vascular bundles with an average tensile strength of 1.90 ± 0.32 GPa, Young's modulus of 91.3 ± 29.7 GPa, and toughness of 25.4 ± 4.5 MJ m^{-3}, which exceed those of the mechanically extracted vascular bundles. This work provides a good reference method for successfully extracting scalable long and undamaged vascular bundles from tough bamboo material.

The structure of a bamboo culm in a transverse section is characterized by numerous vascular bundles embedded in the parenchymatous ground tissue. Through anatomical investigations, it can be found that there are thousands of vascular bundles within a bamboo culm cross-section. Previous studies have conducted mechanical tests on the extracted vascular bundles. However, these tests were limited to part of vascular bundles. Only a few studies have examined the mechanical properties variation of vascular bundles with respect to their layer location within a bamboo culm [17,25]. To characterize bamboo mechanical properties and graded variation within the bamboo culm, it is necessary to identify the relationship between the variation of mechanical properties and the exact location of vascular bundles.

This investigation aims to find the exact gradient variation of the mechanical properties of these continuously distributed vascular bundles within the bamboo culm. This work will provide a basis for the highly processed product's application of bamboo resources and a reference for further study on the trans-scale analysis of the mechanical properties of bamboo.

2. Materials and Methods

2.1. Origin and Sampling of Bamboo Culms

The 4-year-old Moso bamboo *Phyllostachys edulis* was collected from a plantation located in Suqian City, Jiangsu Province, China. Where the bamboo with a breast diameter of 7–9 cm and height of 6–7 m was selected. Every culm was cut into four long segments in the longitudinal direction. These segments were kept for about six months for seasoning.

Three internodes from heights of 1, 3, and 5 m were cut and named as the base, middle, and top sections, respectively. Along the longitudinal direction, each internode was cut into two segments, namely the short part (about 3 cm length) and the long part (about 10 cm length). The short part (Figure 1) was used to observe the location distribution and measure the cross-section area of vascular bundles along the radial direction of the bamboo culm wall. At the same time, the longer part was used to extract vascular bundles and test the mechanical properties.

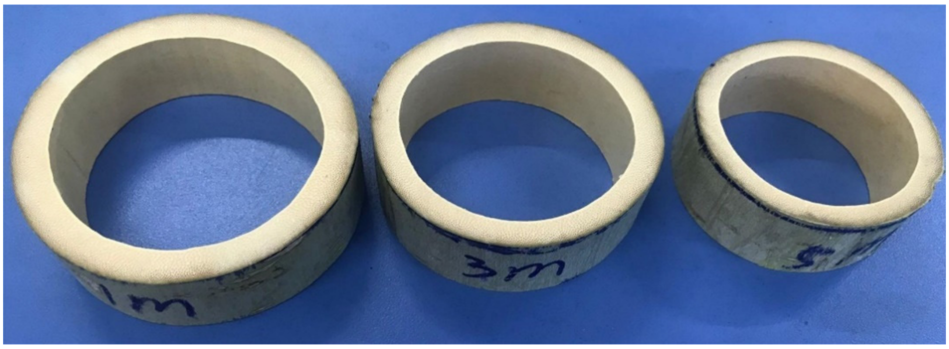

Figure 1. Bamboo rings from different height positions.

2.2. The Vascular Bundles' Precise Location and Area Calculation

The short bamboo ring was divided into 8 equal parts along the clockwise direction, as shown in Figure 2. Within each part, two represented columns of vascular bundles, arranged from the inner to the outer side, were chosen for the vascular bundles' precise localization and observation. Consequently, there were a total of 16 columns of vascular bundles that needed to be observed in this experiment.

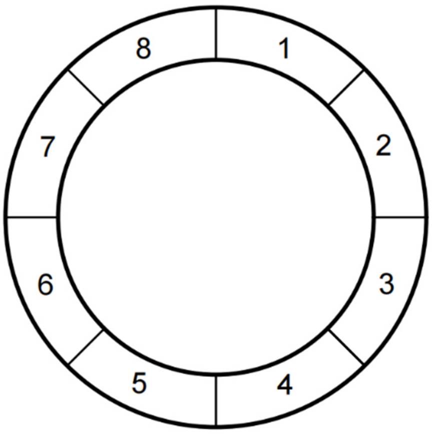

Figure 2. Bamboo ring division.

With the changes in height, the number of vascular bundles decreases steadily from the base to the top. In order to determine the variability of the location of vascular bundles, the location of the scatted vascular bundles in the section plane was described by row and column for comparison. From different height sections, the vascular bundles were divided into 15 rows at the base part, 13 rows at the middle part, and 12 rows at the top part. To determine the location of each vascular bundle along a column, a coordinate system was further established, where the innermost position of the vascular bundle is designated as the origin of coordinates, and the tangential and radial direction are named as the x-axis and R-axis, respectively (Figure 3a). A non-dimensional radius, $\overline{r}$, defined by the distance from the inner surface divided by the culm thickness t, was described as Equation (1):

$$\overline{r} = \frac{(r - r_0)}{t} \quad (1)$$

where r is the radial position of the vascular bundle in bamboo culm, r_0 is the inner surface, t is the culm thickness, $\overline{r} = 0$ corresponds to the inner surface, and $\overline{r} = 1$ to the outer surface.

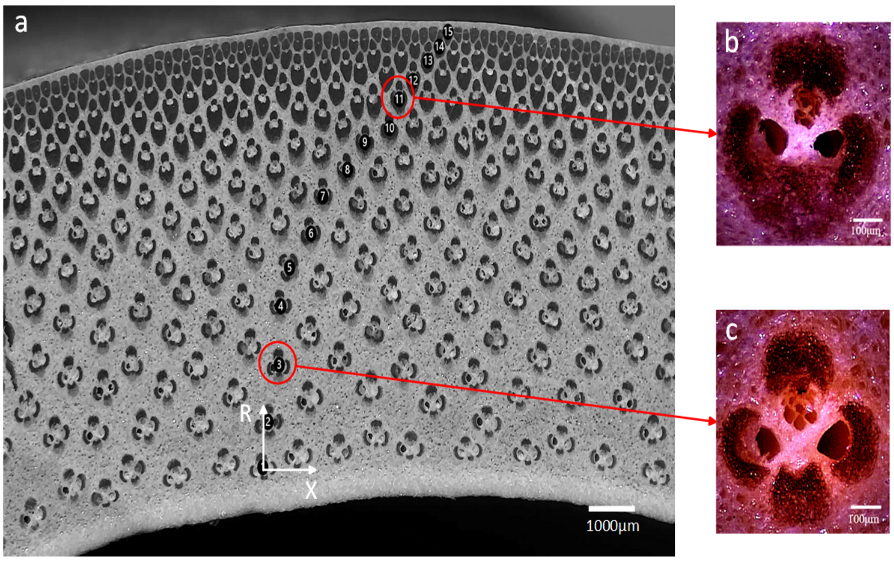

Figure 3. Vascular bundles in bamboo culm: (**a**) location of vascular bundles along a column, number 1–15 means vascular bundle from the inner to the outer periphery of the culm wall. (**b**) semi-open type, and (**c**) open type.

The short bamboo segments in Figure 1 were polished. The targeted vascular bundle photograph was captured using a stereomicroscope. The cross-sectional area of the vascular bundles was measured using the image processing software Digimizer 5.44. The software's built-in image processing tools were employed to capture the outline of the vascular bundle cross-sections, ensuring a distinct differentiation between the vascular bundles and the parenchymatous ground tissue. Points were manually plotted along the boundary of the vascular bundle to measure the cross-sectional area (Figure 4).

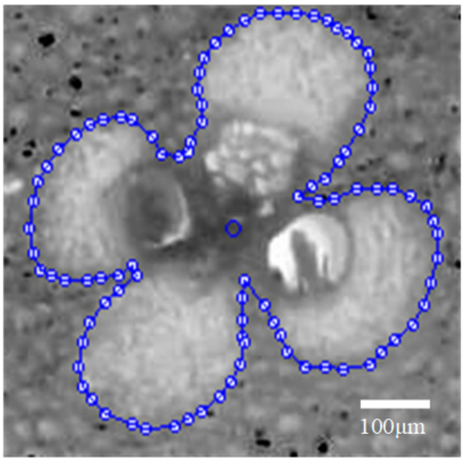

Figure 4. Vascular bundle cross-section area measurement.

2.3. Sample Preparation and Tensile Test

The longer parts of bamboo segments taken from the base, middle, and top internodes were divided into eight equal bamboo strips along the circumferential direction. Following the vascular bundle separation method from Li et al. [26], the prepared bamboo strips were soaked in peroxy formic acid solution (synthesized from a mixture of 30% hydrogen peroxide (Tianjin Damao chemical reagent factory, Tainjin, China) and formic acid (Tianjin Fengboat Chemical reagent Technology Co., Ltd. Tainjin, China) at a mole-to-mole ratio of 1:1, 1% sulfuric acid (Tianjin Fengboat Chemical reagent Technology Co., Ltd. Tainjin, China) was added as a catalyst) for 10 h at a constant temperature of 50 °C, as shown in Figure 5a. Subsequently, the strips were soaked in a 0.5% NaOH (Tianjin Damao chemical reagent factory, Tainjin, China) solution for 10 min and washed with distilled water. In this way, the softened bamboo strip samples can be obtained. Since the treatment was applied to the whole bamboo strip but not thin slices, it can ensure the location of vascular bundles is fixed in the strip. Under a stereomicroscope, parenchymatous ground tissue surrounding the vascular bundles was carefully eliminated with a sharp blade. Finally, all of the vascular bundles from the same column were picked out from the bamboo strip (Figure 5b).

Two strengthening plates, each 0.3 mm thick and 10 mm long, were bonded at both ends of the specimens to protect the specimens from clamping damage (Figure 5c). The gauge length of the specimen was set at 40 mm. A single vascular bundle tensile test was performed longitudinally using a universal tensile test machine (INSTRON5544, Instron, MA, USA) with a 2000 N sensor at a 2 mm min^{-1} displacement rate (Figure 5d). Once the vascular bundle was broken, the fracture morphology was observed by a scanning electron microscope (SEM, JSM-7500F, JEOL, TYO, Japan).

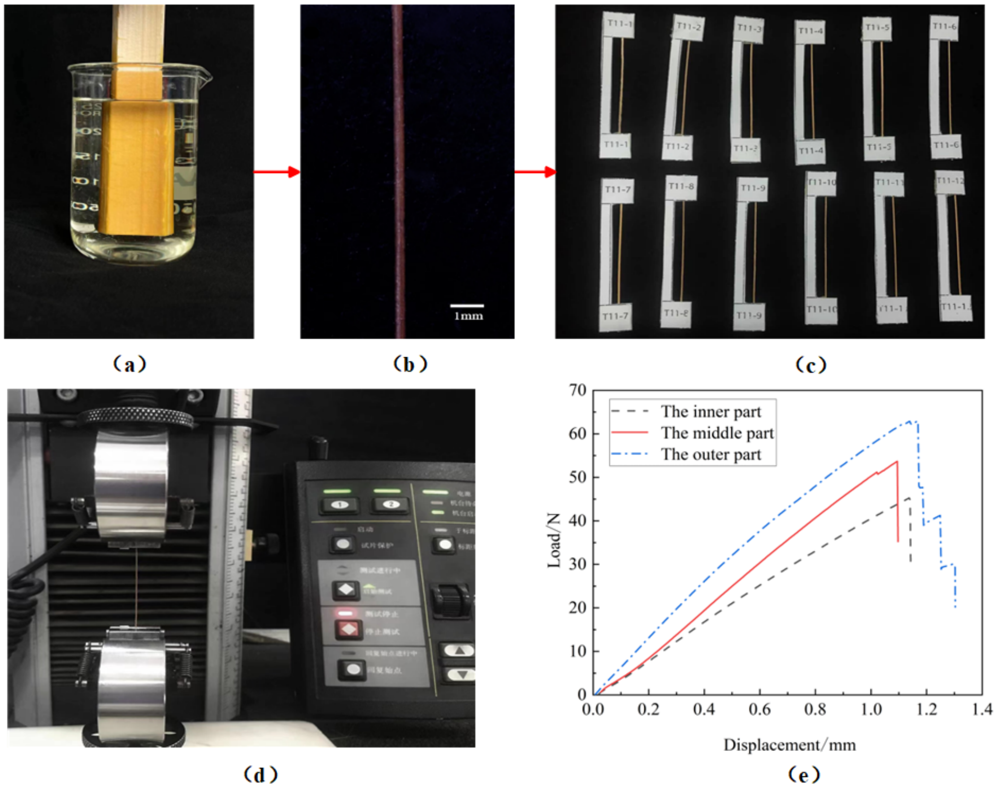

Figure 5. Separation process and tensile test of vascular bundles: (**a**) bamboo strips delignification, (**b**) the isolated vascular bundle, (**c**) preparation of vascular bundle specimen, (**d**) tensile test of single vascular bundle, and (**e**) load–displacement curves of vascular bundle specimen in tension.

During the test, the computer collected data through a force sensor, and the material testing software Bluehill 2.17 plotted the load–displacement curve of the specimen (Figure 5e). Parameters such as Young's modulus, tensile strength, and maximum tensile force of the vascular bundle were obtained from the test results. From the load–displacement curve, the linear segment within the initial elastic deformation segment was selected to calculate Young's modulus of the vascular bundle, and Young's modulus was calculated according to Equation (2). The tensile strength of the vascular bundles was measured as Equation (3):

$$E = \frac{Fl}{\Delta l A} \quad (2)$$

where E is Young's modulus, GPa; F is the tensile force, N; l is the specimen scale distance, mm; Δl is the specimen deformation, mm; and A is the cross-section area of the vascular bundle, mm^2.

$$\sigma_b = \frac{F_{max}}{A} \quad (3)$$

where σ_b is the tensile strength, MPa, and F_{max} is the maximum tensile force, N.

2.4. Data Processing Methods

Statistical analysis software SAS 9.2 was utilized to perform an analysis of variance (ANOVA) on the experimental data. Before performing test F, the normal distribution and homogeneity of variances tests were performed using the graphical method and Levene's test, respectively. The Duncan multiple range test is one kind of the popular multiple comparison procedures in SAS. So, it was applied for mean comparisons to analyze the differences in cross-sectional area and mechanical properties of vascular bundles at various radial positions.

3. Results

3.1. Vascular Bundles Position Distribution within the Bamboo Culm

The distribution pattern of many plants, including succulent leaves, pine cone fruits, and sunflower seeds, follows a golden spiral curve [29]. The distribution of vascular bundles in bamboo culm also exhibits a similar pattern (Figure 3). With the positioning method and coordinate system in Section 2.2 the spatial distribution of vascular bundles within the bamboo culm is shown in Figure 6. The fitted curve along the radial direction can be expressed in exponential form (Equation (4)), and the equations are obtained for the base part, middle part, and top part.

$$\bar{r} = a + be^{cx} \tag{4}$$

where the coefficients in the three height locations are the following:

$$\text{The base part: } a = 0.92,\ \ b = -0.84,\ \ c = -0.53$$

$$\text{The middle part: } a = 1.08,\ \ b = -1.06,\ \ c = -0.38$$

$$\text{The top part: } a = 1.04,\ \ b = -0.98,\ \ c = -0.56$$

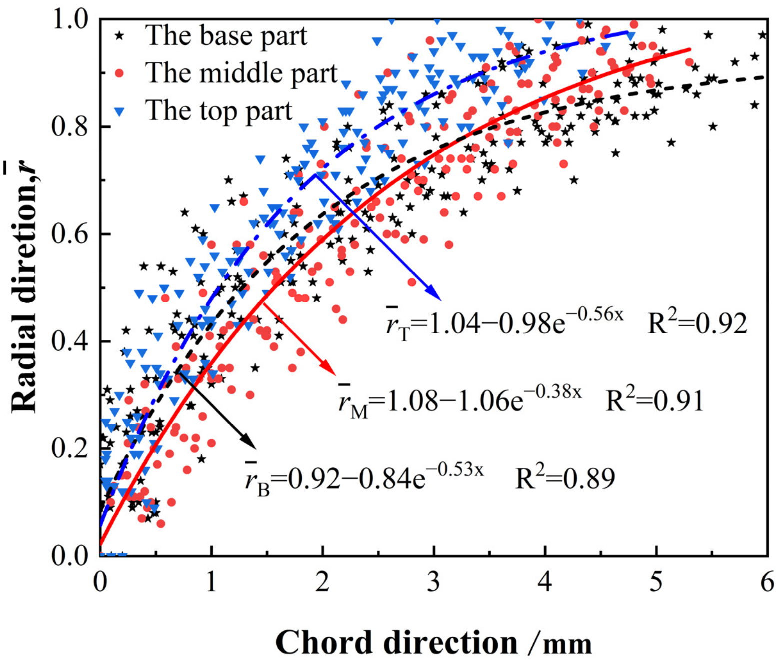

Figure 6. Locate distribution of vascular bundles in bamboo culm.

3.2. The Radial Variation of the Cross-Section Area of Vascular Bundles

The cross-sectional area of the vascular bundles at different positions is shown in Table 1. It can be seen that the range of cross-sectional areas of the vascular bundles within the bamboo culm varies from 0.061 to 0.194 mm^2. The results indicate that the variation in the cross-sectional area of the vascular bundles within the bamboo culm wall is highly significant along the radial direction ($p < 0.01$) but not with height ($p > 0.05$), as shown in Table 2.

Table 1. Test results of vascular bundles.

No.	Cross-Section Area/mm^2			Tensile Strength/MPa			Young's Modulus/GPa		
	Base	Middle	Top	Base	Middle	Top	Base	Middle	Top
1	0.178 ± 0.02 AB	0.171 ± 0.02 BC	0.185 ± 0.02 AB	180.44 ± 41.20 A	215.16 ± 61.07 A	270.78 ± 46.72 A	9.00 ± 1.92 A	11.25 ± 2.18 AB	13.16 ± 2.48 A
2	0.186 ± 0.01 A	0.194 ± 0.01 A	0.191 ± 0.01 A	185.34 ± 58.23 A	226.80 ± 67.30 A	276.56 ± 56.71 A	9.77 ± 2.10 A	10.32 ± 1.46 A	13.29 ± 1.27 A
3	0.185 ± 0.01 A	0.177 ± 0.01 B	0.187 ± 0.01 AB	190.43 ± 58.36 A	226.06 ± 55.71 A	284.02 ± 49.05 A	9.62 ± 1.63 A	10.86 ± 1.56 AB	14.07 ± 1.22 AB
4	0.184 ± 0.01 AB	0.176 ± 0.01 BC	0.179 ± 0.01 B	203.43 ± 65.12 AB	258.78 ± 66.78 AB	283.33 ± 43.63 A	10.64 ± 1.91 AB	11.89 ± 2.04 AB	14.37 ± 1.39 AB
5	0.181 ± 0.01 AB	0.177 ± 0.02 B	0.179 ± 0.01 B	224.44 ± 66.18 ABC	265.47 ± 55.97 AB	286.13 ± 55.59 A	11.2 ± 2.22 AB	12.46 ± 1.92 AB	14.77 ± 1.63 AB
6	0.179 ± 0.01 AB	0.171 ± 0.01 BC	0.167 ± 0.02 C	249.32 ± 89.82 ABC	335.73 ± 87.54 BC	315.96 ± 80.86 A	11.81 ± 2.70 AB	13.86 ± 2.50 AB	17.78 ± 2.41 BC
7	0.175 ± 0.02 AB	0.165 ± 0.01 C	0.169 ± 0.02 C	276.41 ± 83.75 CD	333.33 ± 60.01 BC	337.06 ± 45.70 AB	13.88 ± 3.50 BC	15.06 ± 2.88 BC	19.11 ± 1.57 CD
8	0.173 ± 0.01 B	0.153 ± 0.01 D	0.154 ± 0.02 D	289.47 ± 103.84 DE	391.66 ± 66.23 CD	407.95 ± 110.73 BC	14.93 ± 3.50 C	18.15 ± 3.78 CD	22.01 ± 3.17 D
9	0.161 ± 0.01 C	0.147 ± 0.01 D	0.135 ± 0.01 E	301.24 ±69.44 DE	427.33 ± 93.83 DE	467.57 ± 128.37 CD	15.27 ± 4.00 C	20.61 ± 3.87 DE	25.97 ± 4.89 E
10	0.144 ± 0.02 D	0.131 ± 0.01 E	0.121 ± 0.01 F	357.55 ±89.37 EF	485.88 ± 80.21 E	518.79 ± 169.93 D	20.15 ± 2.87 D	23.76 ± 2.71 E	29.76 ± 5.99 E
11	0.129 ± 0.02 E	0.114 ± 0.01 F	0.104 ± 0.02 G	395.41 ± 103.69 FG	581.84 ± 128.50 F	615.31 ± 182.61 E	21.72 ± 4.43 DE	28.64 ± 5.49 F	35.42 ± 9.68 F
12	0.119 ± 0.01 E	0.096 ± 0.02 G	0.074 ± 0.02 H	438.15 ± 94.46 G	625.88 ± 192.34 F	721.38 ± 215.75 F	24.78 ± 6.59 EF	33.32 ± 8.34 G	44.76 ± 13.68 G
13	0.105 ± 0.01 F	0.061 ± 0.01 H	-	457.56 ±85.60 G	774.10 ± 246.60 G	-	27.18 ± 4.02 F	44.37 ± 14.25 H	-
14	0.095 ± 0.01 G	-	-	557.71 ± 203.73 H	-	-	32.76 ± 9.15 G	-	-
15	0.072 ± 0.02 H	-	-	602.86 ± 215.62 H	-	-	35.72 ± 11.14 G	-	-

Note: $p < 0.01$ means highly significant, $0.01 \leq p < 0.05$ means significant, and $p > 0.05$ means not significant. Different capital letters A, B, C, D, E, F, G, and H indicate significant differences for radial position at 0.05 level according to Duncan's multiple range test.

Table 2. Analysis of variation of vascular bundle cross-sectional area and tensile test results.

Source of Variation	*p*-Values		
	Cross-Section Area	Tensile Strength	Young's Modulus
Radial	<0.001	<0.001	<0.001
Height	0.4267	<0.001	<0.001

Note: $p < 0.01$ means highly significant, $0.01 \leq p < 0.05$ means significant, and $p > 0.05$ means not significant according to test F.

Figure 7 shows the radial variation of the cross-sectional area of a single vascular bundle along the column. The cross-sectional area of single vascular bundles decreases slightly from the inner side to the middle part, with the maximum area near the inner zone decreasing rapidly from the middle part to the outer zone. Overall, the radial variation pattern of the vascular bundle cross-section area can be expressed as Equation (5):

$$A = 0.19 - 8.17e^{5.27\bar{r}} \quad (5)$$

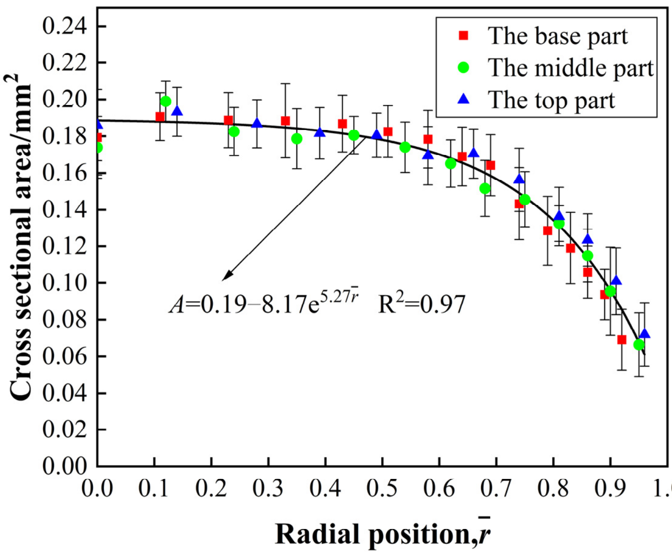

Figure 7. The radial variation of the cross-section area of vascular bundles.

Vascular bundle cross-sectional area variation with radial is strongly related to morphology. There are two types of morphology for vascular bundles in Moso bamboo: semi-open type and open type [25]. The vascular bundles near the inner side of the bamboo culm show an open-type morphology, as shown in Figure 3c. They consist of four independent fiber sheaths, fully differentiated xylem and phloem fractions, which made them nearly the same size. From the middle to the periphery, the vascular bundles show a semi-open-type morphology, with two fiber sheaths gradually diminishing, as shown in Figure 3b. The size of differentiated vessels and sieve tubes also decreases radially, resulting in a rapid reduction in the cross-section area of the vascular bundles.

3.3. Gradient Variation of Vascular Bundle Tensile Properties

The mechanical properties of air-dried Moso bamboo vascular bundles were obtained with the tensile tests, and the test results are shown in Table 1. It shows that the tensile strength of vascular bundles in the base internode, middle internode, and top internode ranged from 180.64 to 602.86 MPa, 215.16 to 774.10 MPa, and 270.78 to 721.38 MPa, respectively. Young's modulus of vascular bundles in the base internode, middle internode, and top internode ranged from 9 to 35.72 GPa, 11.25 to 44.37 GPa, and 13.16 to 44.76 GPa, respectively. Comparing the test results, it can be found that the tensile strength of vascular bundles at the outer side is three times higher than that of the inner side, while Young's modulus at the outer side is nearly three to four times higher than that of the inner side.

3.3.1. Gradient Variation of Tensile Strength

The tensile strength of vascular bundles varies significantly with radial and heights ($p < 0.01$), as shown in Table 2. The change rule of vascular bundle tensile strength with radial at different internodes is shown in Figure 8. It can be seen that the tensile strength of vascular bundles of all three height internodes follow similar trends along the radial direction: the tensile strength of vascular bundles near the inner side of bamboo culm changes slowly, while those from the middle to the outer side increases rapidly and reached to the maximum at the outer periphery. The gradient variation of tensile strength of all three heights can be expressed exponentially as Equation (6):

$$\sigma_{\mathrm{b}}(\bar{r}) = \sigma_{\mathrm{b}0} + Be^{k_1\bar{r}} \tag{6}$$

where the coefficients in the three height locations are the following:

$$\text{The base part: } \sigma_{\mathrm{b}0} = 183.24, \quad B = 4.19, \quad k_1 = 4.99$$

$$\text{The middle part: } \sigma_{\mathrm{b}0} = 215.27, \quad B = 7.63, \quad k_1 = 4.49$$

$$\text{The top part: } \sigma_{\mathrm{b}0} = 267.47, \quad B = 1.82, \quad k_1 = 5.75$$

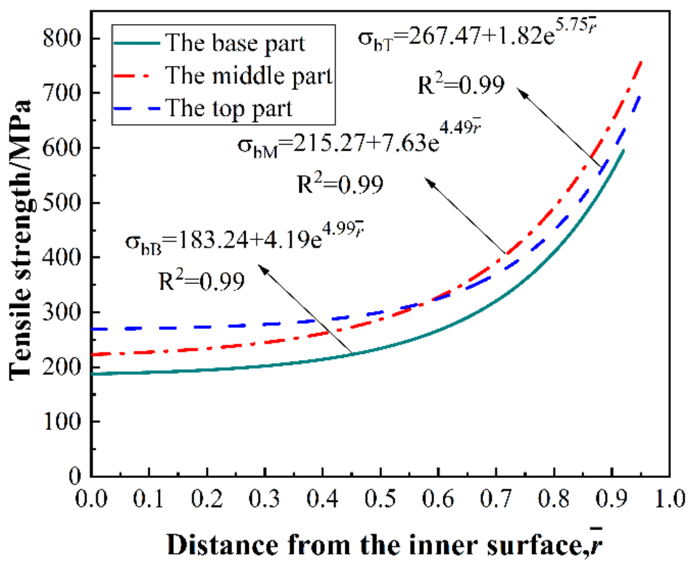

Figure 8. The radial variation of tensile strength of vascular bundles.

A comparison of the tensile strength of vascular bundles at different height positions reveals that both the top and middle parts are stronger than the culm base. In the top and middle of the culm investigated along the culm wall, although the strength in the inner wall of the middle part is smaller than that of the top part, the strength of the middle part increases much more than the top part which made the outer wall of the middle part stronger than that of the top part. With the fitted curves, it can be found that the strength of vascular bundles in the middle and top internodes meet equally at $\bar{r} = 0.58$. Li [7] obtained a similar result to our work; the strength of vascular bundles in the middle and top of the Moso bamboo culm reached an equal level at $\bar{r} = 0.62$. A very interesting observation from these test results is that the ratio of the whole culm wall thickness to the distances from the inner side to the strength equal point are all approximately near the golden ratio (1.618), and this phenomenon has been widely observed in plant structure [30,31].

3.3.2. Gradient Variation of Young's Modulus

The Young's modulus of vascular bundles varied significantly in different radial and height positions within the bamboo culm ($p < 0.01$), as shown in Table 2. Figure 9 shows the variation of Young's modulus of vascular bundles with radial in different culm heights.

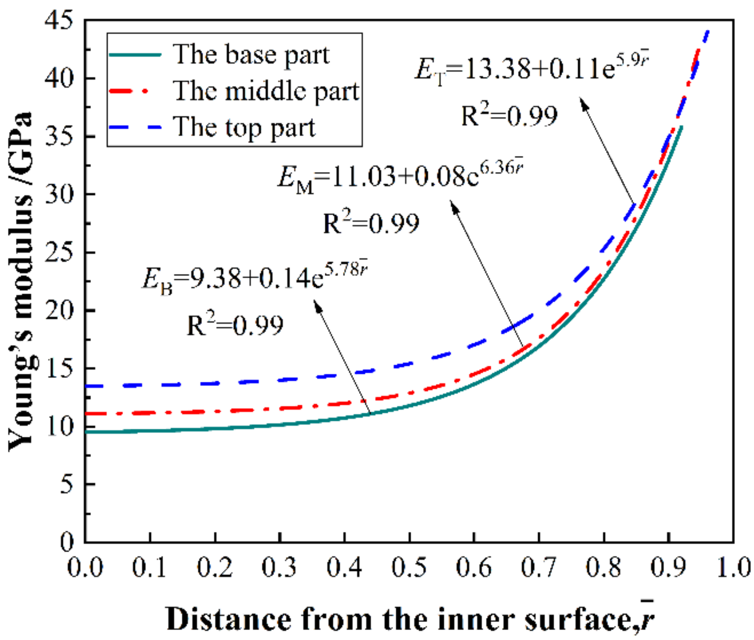

Figure 9. The radial variation of Young's modulus of vascular bundles.

Similar to the feature of tensile strength, the vascular bundles near the outer periphery are stiffer than those near the inner side. The Young's modulus of vascular bundles increases gradually from the inner side to the outer side at different culm heights. The general trend of vascular bundle stiffness as a function of radius is the same for all three positions, which follows an exponential way as in Equation (7):

$$E(\bar{r}) = E_0 + Ce^{k_2\bar{r}} \tag{7}$$

where the coefficients in the three height locations are the following:

$$\text{The base part: } E_0 = 9.38,\ C = 0.14,\ k_2 = 5.78$$

$$\text{The middle part: } E_0 = 11.03,\ C = 0.08,\ k_2 = 6.36$$

$$\text{The top part: } E_0 = 13.38,\ C = 0.11,\ k_2 = 5.9$$

For the vascular bundles at different height locations, it can be seen from Figure 9 that Young's modulus is increased from the base to the top of the culm. Along the thickness direction, due to the different increase rate k_2 in Equation (7), the trends of Young's modulus of vascular bundles at different height culm are different. Finally, Young's modulus approach has nearly the same value at the periphery ($\bar{r} = 1$): 54.71 GPa for the base part, 57.29 GPa for the middle part, and 53.53 GPa for the top part.

3.4. Fracture Mode

The tensile load–displacement curves of bamboo vascular bundles at different wall positions are shown in Figure 5e. Although all of the stress–strain behavior under loading shows approximately linear elastic deformation before reaching the fracture stress, they are broken with different fracture properties. Owing to the variation of shape, size, and concentration of vascular bundles across the internode wall, the vascular bundles are broken into different fracture modes, namely the brittle type and broom-like type.

Figure 10 shows photographs of the vascular bundle samples after tensile testing. From this, it can be found that there are different broken properties in the inner (Figure 10a–c) and outer (Figure 10d–f) culm walls.

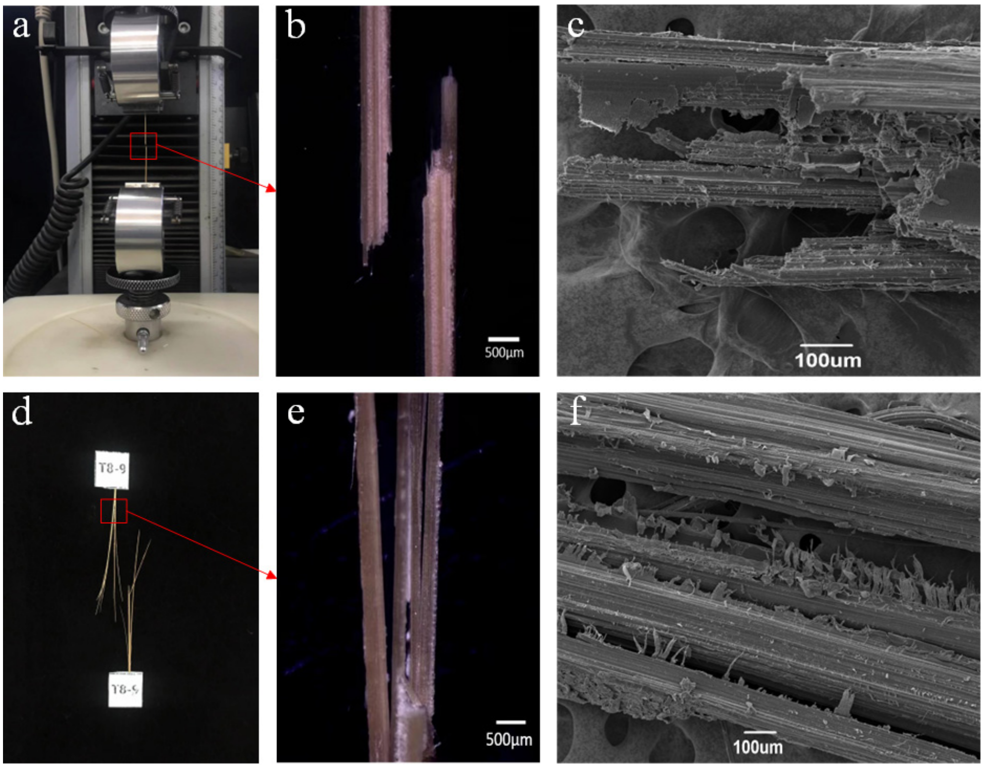

Figure 10. The fracture modes of vascular bundles: (**a**–**c**) fracture modes of inner vascular bundles and (**d**–**f**) fracture modes of outer vascular bundles.

Vascular bundles can be viewed as composite materials made up of sclerenchyma fiber and multi-porous matrix phases. The vascular bundles near the inner side belong to the open-type morphology with a supporting tissue of four sclerenchyma fibers on the sides. With the reason that the area of central multi-porous matrix phases is strikingly larger, but the strength is much weaker than the sclerenchyma sheaths, which made the vascular bundles broken with a brittle type (Figure 10b,c).

Different from the inner vascular bundles, vascular bundles from the middle to the outer side of the bamboo culm show a semi-open-type morphology with the lateral and inner sclerenchyma fiber linked together. The area of multi-porous matrix phases is extremely small and trends to zero on the outer periphery. During the tensile process, the stress–displacement curve shows a linear segment until it reaches the fracture load. The cracks first appear in the weak areas between parenchyma cells and fiber bundles, causing the fiber bundles to gradually separate (Figure 10d–f), with the separated fiber bundles having a smaller area and continuing to sustain the load. Under larger loads, the separated fiber bundles begin to fracture gradually according to the size of their area until the vascular bundle specimen fails as a whole [32]. The fracture shows a staggered decrease in load and made the vascular bundles finally broken with a broom-like type (Figure 10d).

4. Discussion

To investigate the mechanical properties of single vascular bundles in bamboo culm walls, the splitting method was often used to divide the culm wall into several thin slices; then, the single vascular bundles were extracted from thin slices by mechanical or chemical methods. This splitting method has disadvantages and advantages. The advantage is it is easy to extract some contact single vascular bundles. The disadvantage is that it can only obtain some vascular bundles but not all vascular bundles in the culm wall.

Because the extracted vascular bundles from thin slices were measured by their rough but not precise location in the culm wall, it is difficult to find the exact gradient variation of the mechanical properties of these continuously distributed vascular bundles along the bamboo culm wall. Li and Shen [17] divided Moso bamboo strips into six slices to extract single vascular bundles and found that both the vascular bundles' strength and Young's modulus were linearly increased from the inner side to the outer side. Shang et al. [25] divided the vascular bundles into 14 layers to extract single vascular bundles and found that the strength and Young's modulus of the vascular bundles all gradually increased from the inner side to the outer side. From this, we can find that the more layers the strips were peeled, the more exact gradient variation of the mechanical properties of vascular bundles can be obtained.

In this paper, whole long and undamaged vascular bundles were successfully extracted from bamboo culm walls by the chemical delignification methods. This method ensured that the position of the vascular bundles remained unchanged during the extraction process. The test results obtained in this paper are more accurate than previous research in the gradient variation of the mechanical properties of vascular bundles along the culm wall.

The results of Figure 7 indicate that the vascular bundle cross-sectional area exhibited significant variation with radial but not with height. Along the height direction, although the area of vascular bundles was somewhat larger in the base internodes according to absolute position (Table 1), the variation of the area was not obvious according to the relative position, $\bar{r}$. From the analysis results shown in Table 2, it can be found that $P = 0.4267$, which shows that the cross-sectional area of the vascular bundles was not statistically significant along the height direction. Many researchers have come to the same results [25,33].

Bamboo is a fast-growing, cheap, and green resource with superior mechanical and physical properties; it offers great potential as an alternative to wood, plastic, and other materials for structural and product applications. There are approximately 1500 species of bamboo worldwide. In this paper, the Moso bamboo was chosen as a typical representative species to investigate the exact gradient variation of the mechanical properties of the continuously distributed vascular bundles. This work can supply references for other typical bamboo species with different vascular bundle types. Furthermore, a better understanding of the optimal design in natural bamboo will be helpful for designing functionally graded materials with excellent mechanical properties.

5. Conclusions

(1) The radial distribution of vascular bundles in the bamboo culm follows an exponential pattern at different heights.

(2) The cross-section area of vascular bundles in the bamboo culm is larger on the inside and smaller on the outside and decreases exponentially from inside to outside along the radial direction.
(3) Tests showed that the tensile strength of Moso bamboo vascular bundles varied from 180.44 to 774.10 MPa, and Young's modulus varied from 9.00 to 44.76 GPa. Both the vascular bundles' strength and Young's modulus are increased with the exponential gradient variation from the inside to the outer periphery along the culm wall.
(4) The single vascular bundles from different bamboo culm wall positions are broken with different fracture modes. The vascular bundles near the inner side are broken in a brittle manner, while the vascular bundles near the outer side are broken in a broom-like manner.
(5) This work can supply references for other typical bamboo species with different vascular bundle types.

Author Contributions: Conceptualization and supervision, H.L. and Q.Z.; methodology, H.L.; investigation, X.C.; resources, P.L.; formal analysis, Y.X.; writing—original draft preparation, Q.Z.; writing—review and editing, H.L.; project administration, H.L.; funding acquisition, H.L. All authors have read and agreed to the published version of the manuscript.

Funding: This research was funded by a Research Project Supported by the Shanxi Scholarship Council of China, grant number 2021-075, and supported by the Fundamental Research Program of Shanxi Province, grant number 202303021221090.

Data Availability Statement: The original contributions presented in the study are included in the article, further inquiries can be directed to the corresponding author.

Conflicts of Interest: The authors declare no conflicts of interest.

References

1. Xu, D.; He, S.; Leng, W.; Chen, Y.; Wu, Z. Replacing Plastic with Bamboo: A Review of the Properties and Green Applications of Bamboo-Fiber-Reinforced Polymer Composites. *Polymers* **2023**, *15*, 4276. [CrossRef] [PubMed]
2. Zhao, X.; Ye, H.; Chen, F.; Wang, G. Bamboo as a Substitute for Plastic: Research on the Application Performance and Influencing Mechanism of Bamboo Buttons. *J. Clean. Prod.* **2024**, *446*, 141297. [CrossRef]
3. Low, I.M.; Che, Z.Y.; Latella, B.A. Mapping the Structure, Composition and Mechanical Properties of Bamboo. *J. Mater. Res.* **2006**, *21*, 1969–1976. [CrossRef]
4. Osorio, L.; Trujillo, E.; Van Vuure, A.W.; Verpoest, I. Morphological Aspects and Mechanical Properties of Single Bamboo Fibers and Flexural Characterization of Bamboo/ Epoxy Composites. *J. Reinf. Plast. Compos.* **2011**, *30*, 396–408. [CrossRef]
5. Liu, C.; Liu, M.; Liu, W.; Li, Z.; Xu, F. Interlaminar Fracture Property of Moso Bamboo Strips Influenced by Fiber Distributions in Bamboo Internode and Node. *Compos. Struct.* **2022**, *294*, 115777. [CrossRef]
6. Wegst, U.G.K.; Bai, H.; Saiz, E.; Tomsia, A.P.; Ritchie, R.O. Bioinspired Structural Materials. *Nat. Mater.* **2015**, *14*, 23–36. [CrossRef] [PubMed]
7. Li, H.B. Trans-Scale Analysis of the Mechanical Properties of Moso Bamboo. Ph.D. Thesis, Xi'an Jiaotong University, Xian, China, 2012.
8. Wang, D.; Lin, L.; Fu, F. Fracture Mechanisms of Moso Bamboo (*Phyllostachys pubescens*) under Longitudinal Tensile Loading. *Ind. Crops Prod.* **2020**, *153*, 112574. [CrossRef]
9. Wang, X.; Chen, X.; Huang, B.; Chen, L.; Fang, C.-H.; Ma, X.; Fei, B. Gradient Changes in Fiber Bundle Content and Mechanical Properties Lead to Asymmetric Bending of Bamboo. *Constr. Build. Mater.* **2023**, *395*, 132328. [CrossRef]
10. Gao, X. Structural and Mechanical Properties of Bamboo Fiber Bundle and Fiber/Bundle Reinforced Composites: A Review. *J. Mater. Res. Technol.* **2022**, *19*, 1162–1190. [CrossRef]
11. Han, S.; Xu, H.; Chen, F.; Wang, G. Construction Relationship between a Functionally Graded Structure of Bamboo and Its Strength and Toughness: Underlying Mechanisms. *Constr. Build. Mater.* **2023**, *379*, 131241. [CrossRef]
12. Sun, H.; Li, H.; Dauletbek, A.; Lorenzo, R.; Corbi, I.; Corbi, O.; Ashraf, M. Review on Materials and Structures Inspired by Bamboo. *Constr. Build. Mater.* **2022**, *325*, 126656. [CrossRef]
13. Ghavami, K.; Rodrigues, C.S.; Paciornik, S. Bamboo: Functionally Graded Composite Material. *Asian J. Civ. Eng. Build. Hous.* **2003**, *4*, 1–10.
14. Xu, H.; Zhang, Y.; Wang, J.; Li, J.; Zhong, T.; Ma, X.; Wang, H. A Universal Transfer-Learning-Based Detection Model for Characterizing Vascular Bundles in *Phyllostachys*. *Ind. Crops Prod.* **2022**, *180*, 114705. [CrossRef]
15. Amada, S.; Ichikawa, Y.; Munekata, T.; Nagase, Y.; Shimizu, H. Fiber Texture and Mechanical Graded Structure of Bamboo. *Compos. Part B Eng.* **1997**, *28*, 13–20. [CrossRef]

16. Amada, S.; Untao, S. Fracture Properties of Bamboo. *Compos. Part B Eng.* **2001**, *32*, 451–459. [CrossRef]
17. Li, H.; Shen, S. The Mechanical Properties of Bamboo and Vascular Bundles. *J. Mater. Res.* **2011**, *26*, 2749–2756. [CrossRef]
18. Nogata, F.; Takahashi, H. Intelligent Functionally Graded Material: Bamboo. *Compos. Eng.* **1995**, *5*, 743–751. [CrossRef]
19. Shao, Z.-P.; Fang, C.-H.; Huang, S.-X.; Tian, G.-L. Tensile Properties of Moso Bamboo (*Phyllostachys pubescens*) and Its Components with Respect to Its Fiber-Reinforced Composite Structure. *Wood Sci. Technol.* **2010**, *44*, 655–666. [CrossRef]
20. Chen, K.; Long, L.C. Analysis of the Effects of Fiber Gradient Distribution on the Mechanical Properties of Moso Bamboo. *Appl. Mech. Mater.* **2014**, *590*, 13–18. [CrossRef]
21. Zhang, X.; Li, J.; Yu, Z.; Yu, Y.; Wang, H. Compressive Failure Mechanism and Buckling Analysis of the Graded Hierarchical Bamboo Structure. *J. Mater. Sci.* **2017**, *52*, 6999–7007. [CrossRef]
22. Dixon, P.G.; Gibson, L.J. The Structure and Mechanics of Moso Bamboo Material. *J. R. Soc. Interface* **2014**, *11*, 20140321. [CrossRef] [PubMed]
23. Xu, H.; Li, J.; Ma, X.; Yi, W.; Wang, H. Intelligent Analysis Technology of Bamboo Structure. Part II: The Variability of Radial Distribution of Fiber Volume Fraction. *Ind. Crops Prod.* **2021**, *174*, 114164. [CrossRef]
24. Wang, F.; Shao, Z. Study on the Variation Law of Bamboo Fibers' Tensile Properties and the Organization Structure on the Radial Direction of Bamboo Stem. *Ind. Crops Prod.* **2020**, *152*, 112521. [CrossRef]
25. Shang, L.; Liu, X.; Jiang, Z.; Tian, G.; Yang, S. Variation in Tensile Properties of Single Vascular Bundles in Moso Bamboo. *For. Prod. J.* **2021**, *71*, 246–251. [CrossRef]
26. Li, Z.; Chen, C.; Xie, H.; Yao, Y.; Zhang, X.; Brozena, A.; Li, J.; Ding, Y.; Zhao, X.; Hong, M.; et al. Sustainable High-Strength Macrofibres Extracted from Natural Bamboo. *Nat. Sustain.* **2022**, *5*, 235–244. [CrossRef]
27. Fu, J.; Zhang, X.; Yu, C.; Guebite, G.M.; Cavaco-Paulo, A. Bioprocessing of Bamboo Materials. *Fibres Text. East. Eur.* **2012**, *20*, 13–19.
28. Li, J.; Lian, C.; Wu, J.; Zhong, T.; Zou, Y.; Chen, H. Morphology, Chemical Composition and Thermal Stability of Bamboo Parenchyma Cells and Fibers Isolated by Different Methods. *Cellulose* **2023**, *30*, 2007–2021. [CrossRef]
29. Minarova, N. The Fibonacci Sequence: Nature's Little Secret. *CRIS-Bull. Cent. Res. Interdiscip. Study* **2014**, *2014*, 7–17. [CrossRef]
30. Zeng, L.; Wang, G. Modeling Golden Section in Plants. *Prog. Nat. Sci.* **2009**, *19*, 255–260. [CrossRef]
31. Sun, Z.; Cui, T.; Zhu, Y.; Zhang, W.; Shi, S.; Tang, S.; Du, Z.; Liu, C.; Cui, R.; Chen, H.; et al. The Mechanical Principles behind the Golden Ratio Distribution of Veins in Plant Leaves. *Sci. Rep.* **2018**, *8*, 13859. [CrossRef]
32. Li, Z.; Chen, C.; Mi, R.; Gan, W.; Dai, J.; Jiao, M.; Xie, H.; Yao, Y.; Xiao, S.; Hu, L. A Strong, Tough, and Scalable Structural Material from Fast-Growing Bamboo. *Adv. Mater.* **2020**, *32*, 1906308. [CrossRef] [PubMed]
33. Tsuyama, T.; Hamai, K.; Kijidani, Y.; Sugiyama, J. Quantitative Morphological Transformation of Vascular Bundles in the Culm of Moso Bamboo (*Phyllostachys pubescens*). *PLoS ONE* **2023**, *18*, e0290732. [CrossRef] [PubMed]